

# Development of Thomson Scattering Measurement System for Upstream Plasmas in the NAGDIS-II Device<sup>\*)</sup>

Hiroki TAKANO<sup>1)</sup>, Hiroshi OHSHIMA<sup>1)</sup>, Shin KAJITA<sup>2)</sup>, Hirohiko TANAKA<sup>1)</sup>  
and Noriyasu OHNO<sup>1)</sup>

<sup>1)</sup>Graduate School of Engineering, Nagoya University, Furo-cho, Chikusa-ku, Nagoya 464-8603, Japan

<sup>2)</sup>Institute of Materials and System for Sustainability, Nagoya University, Furo-cho, Chikusa-ku, Nagoya 464-8603, Japan

(Received 27 September 2018 / Accepted 9 December 2018)

A new laser Thomson scattering (LTS) measurement system in the upstream region of the linear plasma device NAGDIS-II is established in addition to the recently introduced LTS in the downstream. Further, horizontal distributions of the electron temperature and electron density were compared with those obtained from the Langmuir probe, indicating plasma disturbance due to the insertion of the probe head. We discuss the variation of the electron energy distribution function at upstream and downstream in the recombining plasma.

© 2019 The Japan Society of Plasma Science and Nuclear Fusion Research

Keywords: laser Thomson scattering, NAGDIS-II, recombining plasma, Langmuir probe, electron energy distribution function

DOI: 10.1585/pfr.14.2405031

## 1. Introduction

In future fusion reactors, one of the issues to be solved is the high heat flux to the divertor plates [1, 2]. Usage of detached recombining plasma, which vanishes the plasma by interacting with neutrals, is regarded as one of the methods to resolve this issue [3, 4]. An accurate measurement method is necessary to clarify the underlying physics such as atomic and molecular processes and transport process. However, it is known that Langmuir probes disturb plasmas and the probe current-voltage characteristics are strongly affected by fluctuating plasma potential in detached plasmas [5]. Passive spectroscopy always has an issue in the line integrated effect, although the accuracy of passive spectroscopy measurement of recombining plasma has been improved by incorporating radiation capture into the calculation of collisional-radiative model [6]. Laser Thomson scattering (LTS) is known as a reliable method to measure electron density ( $n_e$ ) and electron temperature ( $T_e$ ) even in recombining plasmas. The LTS method has been used in various plasma devices, e.g., Pilot-PSI [7], Magnum-PSI [8], PSI-2 [9], NAGDIS-II [10], and other devices [11, 12].

In this study, we have established an LTS measurement system in the upstream region of the linear plasma device NAGDIS-II, in addition to another LTS system developed in the downstream region [10]. These systems enable us to obtain reliable plasma parameters in upstream and downstream and to discuss the scale length of plasma parameters along the magnetic field without the disturbance. Furthermore, a comparison of the plasma parameters with

those obtained by Langmuir probes and the upstream LTS system will be shown. The variation of electron energy distribution function (EEDF) in recombining plasma at upstream and downstream will also be presented.

## 2. Experimental Setup

Figure 1 shows a schematic view of NAGDIS-II (NAGoya Divertor Simulator-II), where length and diameter is 2.5 and 0.18 m, respectively. The magnetic field is made by 20 solenoidal magnetic coils and the strength is up to 0.25 T. The high-density plasma is produced by DC plasma source made by a LaB<sub>6</sub> disc cathode, which is heated by a carbon heater with approximately 3 kW. The cathode chamber and a hollow anode with a diameter of 24 mm are separated by the intermediate floating electrode having an inner diameter of 20 mm. Recombining plasma is produced by supplying additional neutral gas

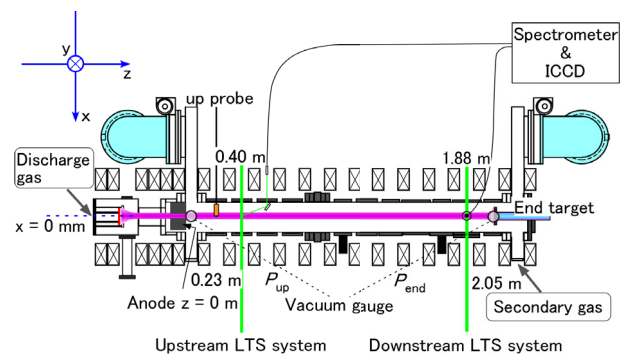


Fig. 1 Schematic of NAGDIS-II with the position of LTS systems and Langmuir probes.

author's e-mail: takano.hiroki@i.mbox.nagoya-u.ac.jp

<sup>\*)</sup> This article is based on the presentation at the 12th International Conference on Open Magnetic Systems for Plasma Confinement (OS2018).

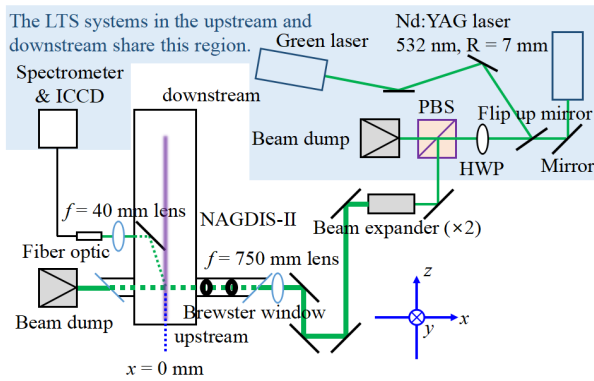


Fig. 2 Schematic of LTS measurement system for upstream.

to increase neutral pressure. The NAGDIS-II has three Langmuir probes, which can measure the horizontal distribution of plasma parameters. In this paper, we use the probe located at 0.23 m downstream from the anode. The downstream LTS system is located approximately 0.16 m in front of the end target ( $y = 2.05$  m).

The position of the LTS system in the upstream is approximately 0.40 m away from the anode (see Fig. 1). Figure 2 shows the optical system of the upstream LTS system. A part of the optical system is shared with the downstream LTS system. The second harmonic (wavelength of 532 nm) of an Nd:YAG laser (Continuum: Surelite II-10) is used having a pulse width of 5-6 ns, pulse energy of  $\sim 0.3$  J, and repetition rate of 10 Hz. After the polarization direction of the laser is changed by a half wave plate (HWP), the polarizing beam splitter (PBS) separates polarization components. The diameter of the laser is doubled by a beam expander and then the laser beam is focused with a lens ( $f = 750$  mm) to increase the energy intensity of the laser at the center of the vacuum vessel.

The collected scattered light is transferred through an optical fiber bundle (core dia.  $230 \mu\text{m}$ , cladding dia.  $250 \mu\text{m}$ ,  $\text{NA} = 0.2$ ), which has 23 channels, to a spectrometer (Bunkoukeiki: FLP-200VPH-P) and Gen-III ICCD camera (Andor: iStar) [13]. The spectrometer has a volume phase holographic grating ( $2600 \text{ mm}^{-1}$ ). Different from the downstream LTS system, there exists no viewing port above the laser beam path in the upstream region. There is a viewing port located at 154 mm downstream side. By installing a mirror inside the vacuum vessel from the viewing port, the scattered laser light at an angle of approximately 60 degrees against the direction of the laser beam path can be collected via the mirror and  $f = 40$  mm lens. We use the same spectrometer used in the downstream LTS, where the fibers are switched between the upstream and downstream LTS measurement.

### 3. Results and Discussion

#### 3.1 Comparison with electrostatic probes

Figure 3 (a) shows the spectrum of the upstream LTS

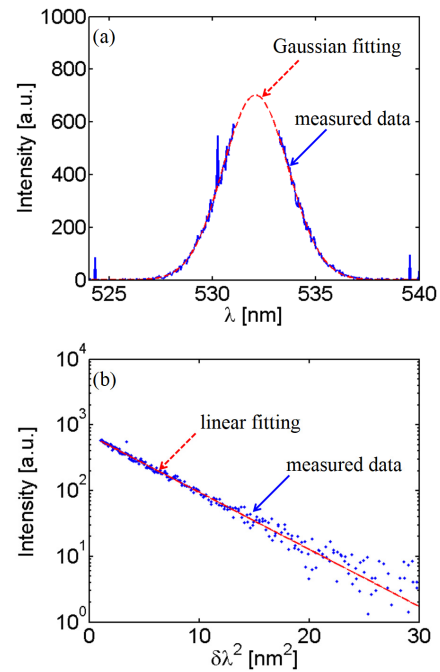


Fig. 3 (a) LTS spectrum of upstream plasma fitted by a single Gaussian curve. (b) EEDF of upstream plasma and linear fitting curve after taking common logarithm for “Intensity”.  $\delta\lambda^2$  means squared shifted wavelength from the spectrum center.

at the plasma center. In this study, we use pure helium plasma. In Fig. 3, the discharge current  $I_d$  was 60 A when the discharge voltage  $V_d$  is 84 V. The neutral gas pressure at the upstream  $P_{\text{up}}$ , and downstream region  $P_{\text{end}}$ , was 3.6 and 14.7 mTorr respectively. The EEDF was deduced from the spectrum by removing stray light and background signals. From the LTS spectrum,  $T_e$  and  $n_e$  is estimated to be 4.5 eV and  $2.4 \times 10^{19} \text{ m}^{-3}$ , respectively. Here,  $n_e$  is calculated from Rayleigh scattered of  $\text{N}_2$  gas.

Figure 4 shows the horizontal distributions of  $T_e$  and  $n_e$  obtained from the upstream LTS and comparison with those measured by the nearest Langmuir probe. The horizontal direction is indicated by the  $x$ -axis, where LTS measurements are made on one side (right) with respect to the plasma center, while the probes are inserted on the opposite side (left), as shown in Figs. 1 and 2. Here, plasma center was determined as the position that has a maximum  $n_e$  measured with the LTS.

In order to investigate plasma disturbance due to the probe insulation shaft (alumina tube,  $\text{Al}_2\text{O}_3$ ), we conducted Langmuir probe measurements with two different diameters; thick and thin probes. Here, “thick probe” has a 4 mm diameter alumina tube, while “thin probe” is 2 mm. The diameter and length of the tungsten electrode are 0.5 and  $\sim 2$  mm, respectively. In the measurements using the thick and thin probes,  $V_d$  are 141 V and 119 V respectively.  $I_d$  are both 20 A.

From Figs. 4 (a) and (b), at  $x \leq -10$  mm, it is found

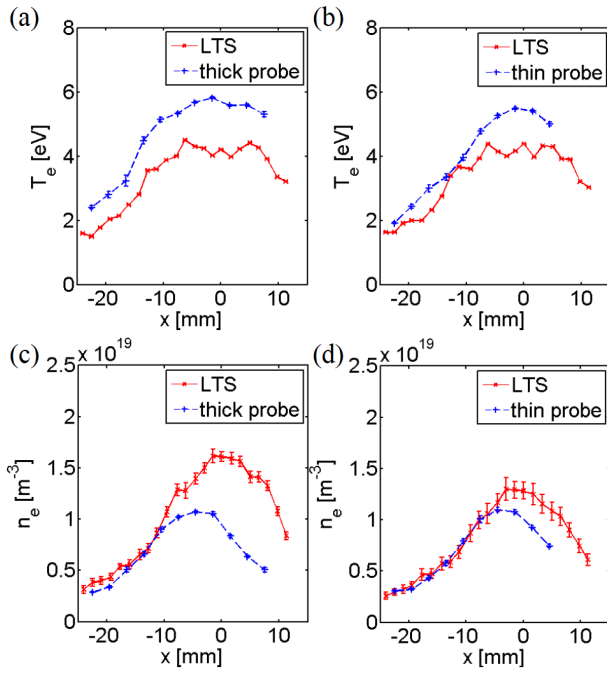


Fig. 4 Horizontal distributions of the upstream LTS system (solid line) comparing  $T_e$  with (a) thick probe, and (b) thin probe. The  $n_e$  measurements are compared with (c) thick probe, and (d) thin probe.

that  $T_e$  measured by the thin probe is closer to  $T_e$  obtained from the LTS system than by the thick probe. In Figs. 4 (c) and (d),  $n_e$  measured by the thin probe matches  $n_e$  by the LTS system at  $x \leq -5$  mm, while  $n_e$  measured by the thick probe matches  $n_e$  by the LTS system only at  $x \leq -10$  mm. At  $x \geq -10$  mm, both probes underestimate  $n_e$  and the peak positions shift toward the  $-x$  direction. The  $n_e$  measurements with the thin and thick probes are  $\sim 28\%$  and  $\sim 45\%$  lower than  $n_e$  measured with the LTS at  $x = 0$  mm, respectively. This would be attributed to the plasma disturbance due to the existence of the probe shaft inside the plasma column near the plasma source ( $x \geq -10$  mm).

These results mean that the thin probe gives smaller disturbance to the plasma than the thick one. However, even by using the thin probe with a diameter of 2 mm, the plasma center cannot be accurately measured due to the disturbance. This result indicates that LTS is necessary to accurately measure the horizontal plasma parameters in the upstream region.

### 3.2 Comparison between upstream and downstream LTS measurements

Figure 5 shows the horizontal distributions of  $T_e$  and  $n_e$  measured with the LTS system in the upstream and downstream region. In the ionizing plasma ( $I_d = 30$  A,  $V_d = 110$  V,  $P_{up} = 2.5$  mTorr, and  $P_{end} = 2.8$  mTorr),  $n_e$  and  $T_e$  at the plasma center in the upstream are  $1.8 \times 10^{19} \text{ m}^{-3}$  and 3.8 eV. On the other hand,  $n_e$  and  $T_e$  in

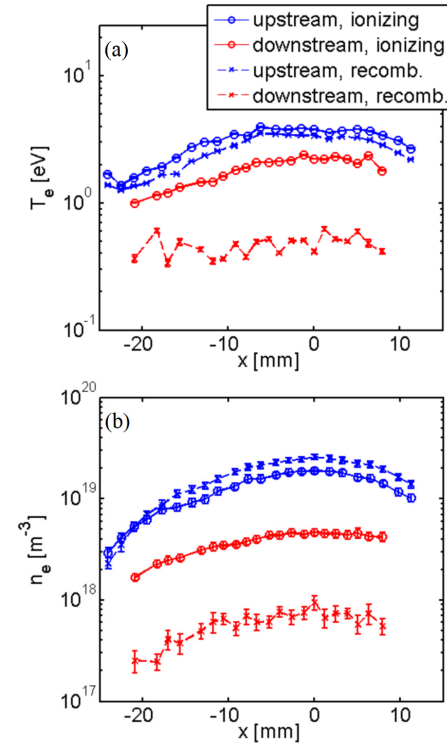


Fig. 5 Comparison of the horizontal distribution of (a)  $T_e$  and (b)  $n_e$  measured with upstream and downstream LTS system in ionizing (solid line) and recombining (dashed line) plasma conditions.

the downstream are  $4.7 \times 10^{18} \text{ m}^{-3}$  and 2.2 eV. Considering static plasma pressure  $P_s$ , defined by the product of  $n_e$  and  $T_e$ , the  $P_s$  is reduced to 14% from upstream to downstream. By changing from ionizing plasma to recombining plasma ( $I_d = 30$  A,  $V_d = 114$  V,  $P_{up} = 3.3$  mTorr, and  $P_{end} = 9.8$  mTorr),  $n_e$  increases by  $\sim 37\%$ , and  $T_e$  slightly drops in the upstream. On the other hand, in the downstream,  $T_e$  drops around 0.5 eV, and  $n_e$  becomes  $9.5 \times 10^{17} \text{ m}^{-3}$  at the plasma center. The  $P_s$  significantly decreases to 0.45% from upstream to downstream because of plasma momentum loss due to a three-body recombination process.

### 3.3 Two different temperature components

In the previous study, it was mentioned that two electron temperature components existed when the plasma state was in the transition from ionizing to recombining plasmas [10], suggesting that the two temperature components were attributed to fluctuations of plasma parameters. Figure 6 shows LTS spectrum and EEDF of downstream at  $P_{end} = 6.5$  mTorr, like the plasma state mentioned above. In Fig. 6 (b), we can recognize that the EEDF gradient has two different inclined angles, implying that there are two electron temperature components. Thus, we applied double Gaussian fitting to the LTS spectrum (see Fig. 6). From double Gaussian fitting,  $n_e$  and  $T_e$  of the high electron tem-

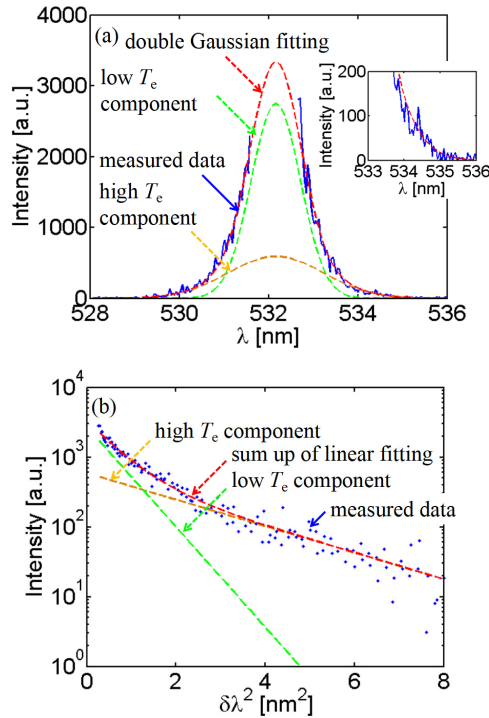


Fig. 6 (a) LTS spectrum and (b) EEDF in downstream plasma. The position is at the center of plasma ( $x = 0$  mm).  $I_d = 30$  A,  $V_d = 113$  V,  $P_{up} = 2.9$  mTorr,  $P_{end} = 6.5$  mTorr.

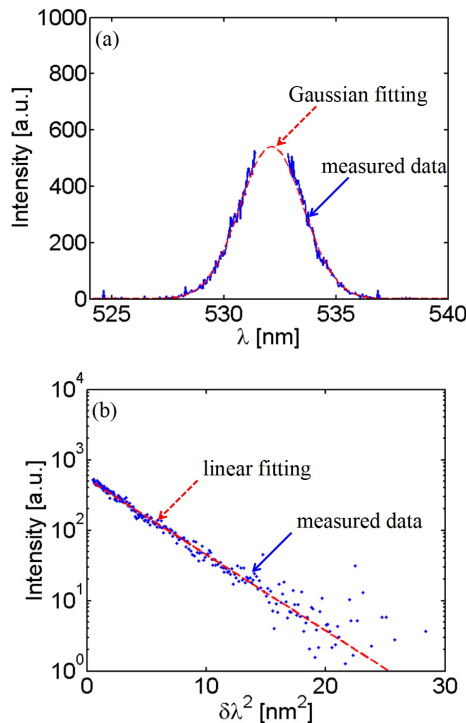


Fig. 7 (a) LTS spectrum with single Gaussian fitting curve and (b) EEDF in upstream plasma. The position is at the center of plasma ( $x = 0$  mm). The experimental condition is the same as Fig. 6.

perature component are  $1.9 \times 10^{18} \text{ m}^{-3}$  and 1.0 eV respectively, while those of the low electron temperature component are  $4.6 \times 10^{18} \text{ m}^{-3}$  and 0.27 eV respectively. On the other hand, in the upstream spectrum and EEDF, no two temperature components are observed, as shown in Fig. 7. This means that the fluctuation of plasma parameters exists only in the downstream of the recombining plasma. In fact, in the multipoint measurement, large fluctuation at the frequency of several kilohertz was considered to be localized in the axial direction [14]. Currently, we are investigating the time evolution of the plasma parameters by applying conditional averaging technique to the LTS and Langmuir probe measurements.

## 4. Conclusion

In this study, we established the LTS system at the upstream of NAGDIS-II device and obtained the plasma parameters,  $T_e$  and  $n_e$ , by using the LTS spectrum. We found that the plasma parameters measured by the thin probe are closer to those measured by the LTS system than by the thick probe. However, even small plasma disturbance due to the thin probe overestimates  $T_e$ ;  $\sim 23\%$  and underestimates  $n_e$ ;  $\sim 28\%$  at the center of the plasma. A comparison of plasma parameters in downstream shows the reduction rate of the static plasma pressure  $P_s$  from upstream to downstream varies by 14% to 0.45% as ionizing plasma is changed to recombining plasma. We also found that two different temperature components [10] exists only in the downstream region of recombining plasmas.

## Acknowledgments

This work was partially supported by JSPS KAKENHI (16H02440, 16H06139), NIFS Collaboration Research program (NIFS17KUGM120, NIFS17KUGM130), and NINS program of Promoting Research by Networking among Institutions (01411702).

- [1] A. Herrmann *et al.*, Plasma Phys. Control. Fusion **37**, 14 (1995).
- [2] K. Tokunaga *et al.*, J. Nucl. Mater. **212-215**, 1323 (1994).
- [3] N. Ohno *et al.*, Nucl. Fusion **41**, 8 (2001).
- [4] S. Kajita *et al.*, Phys. Plasmas **24**, 073301 (2007).
- [5] N. Ohno *et al.*, Contrib. Plasma Phys. **41**, 473 (2001).
- [6] S. Kajita *et al.*, Phys. Plasmas **25**, 063303 (2018).
- [7] H.J. van der Meiden *et al.*, Rev. Sci. Instrum. **79**, 013505 (2008).
- [8] H.J. van der Meiden *et al.*, Rev. Sci. Instrum. **83**, 123505 (2012).
- [9] M. Hubeny *et al.*, Nucl. Mater. Energy **12**, 1253 (2017).
- [10] H. Ohshima *et al.*, Plasma Fusion Res. **13**, 1201099 (2018).
- [11] B. Vincent *et al.*, Plasma Sources Sci. Technol. **27**, 055002 (2018).
- [12] K.Y. Lee *et al.*, Rev. Sci. Instrum. **89**, 013508 (2018).
- [13] S. Kajita *et al.*, Phys. Plasmas **24**, 073301 (2017).
- [14] H. Tanaka *et al.*, Plasma Phys. Control. Fusion **60**, 075013 (2018).